RESEARCH

ATM-Mediated translocation of RanBPM regulates DNA damage response by stabilizing p21 in non-small cell lung cancer cells

Tanggang Deng[1,2] · Lin Xie[1,2] · Chen Xiaofang[1] · Zhenbin Zhang[1,2] · Yugang Xiao[1,2] · Yuchong Peng[1,2] · Linglong Yin[1,2] · Yongming Fu[1,2] · Xiong Li[1,2,3,4]

Abstract

Purpose Platinum-based chemotherapy remains a standard-of-care for most patients with advanced non-small cell lung cancer (NSCLC). DNA damage response (DDR) induced by platinum or Etoposide activated a panel of cell cycle-regulatory proteins including p21 through p53 pathway. Previous studies have reported that RanBPM has been involved in various cellular processes such as DDR by interacting with multiple proteins. However, the underlying mechanism remains unclear.

Methods NSCLC tissue microarrays were used for assessing the expression of RanBPM by immunohistochemical staining. The roles of RanBPM in the DDR of NSCLC progression was examined in in vitro cell lines and in vivo animal models. The regulation of RanBPM on protein stability and ubiquitination levels were investigated by immunoblots and in vivo ubiquitylation assay.

Results The level of p21 or RanBPM is lower in NSCLC than non-malignant tissues and has a highly positive correlation. Mechanistically, RanBPM protein physically interacts with p21, and RanBPM deubiquitinates p21 by recruiting a deubiquitinase USP11 to maintain protein stability of p21. RanBPM silencing significantly decreased p21 protein level. Conversely, RanBPM overexpression led to the accumulation of endogenous p21 protein regardless of p53 status. Functionally, RanBPM regulates DDR in a p21-dependent manner. Furthermore, DNA damage significantly promoted the nuclear translocation of RanBPM protein through ATM signaling pathways.

Conclusion RanBPM is a novel regulator of P21 protein stability, and plays a critical role in the regulation of DDR.

Keywords RanBPM · p21 · Deubiquitination · USP11 · DNA damage

Tanggang Deng and Lin Xie contributed equally to this work.

✉ Tanggang Deng
dengtanggang@163.com

✉ Xiong Li
lixiong@gdpu.edu.cn

1 Center for Clinical Precision Pharmacy, The First Affiliated Hospital, Guangdong Pharmaceutical University, 19 Nonglinxia Road, Yuexiu District, Guangzhou, Guangdong, China

2 Clinical Pharmacy, The First Affiliated Hospital, Guangdong Pharmaceutical University, Guangzhou, China

3 NMPA Key Laboratory for Technology Research and Evaluation of Pharmacovigilance, Guangdong Pharmaceutical University, Guangzhou, China

4 School of Basic Medical Sciences, Guangdong Pharmaceutical University, Guangzhou, China

1 Introduction

Lung cancer is a frequently diagnosed malignancy with the second morbidity and the highest mortality worldwide. According to the latest Global Cancer Statistics 2020, lung cancer accounts for 11.4% of the total new cases, and for 18% of the total cancer deaths [1]. Non-Small Cell Lung Cancer (NSCLC) is the most common type of lung cancer, accounting for 80–85% of all cases [2]. Based on the histological features, NSCLC is further divided into lung adenocarcinomas, squamous cell carcinoma and large cell carcinoma [3]. Platinum-based chemotherapy is the standard-of-care for NSCLC patients before or after surgery, or alongside radiotherapy, or for the advanced NSCLC patients [4]. Chemotherapy-caused DNA damage activates a series of DNA damage response (DDR), including the activation of ATM/ATR, and then triggers the downstream cell processes, such as cell cycle arrest, DNA damage repair, cell

senescence or apoptosis [5]. However, cancer cells will develop drug-resistance after a period of treatment. Therefore, it is urgently required to reveal the molecular mechanism of drug resistance of NSCLC, identify the predictive diagnostic biomarkers, and develop the new therapies.

RanBPM, known as RanBP9, is a ubiquitous, evolutionarily conserved scaffold protein, which is localized in both cytoplasm and nucleus [6]. Previous studies have demonstrated that RanBPM interacts with multiple proteins that involved in various cellular processes, such as cell adhesion and migration, DDR and signal transduction [7–9]. RanBPM-deficient mice show early perinatal lethality and sterility [10, 11]. RanBPM has also been identified as a critical regulator of protein stabilization, and regulates diverse biological functions through protein interaction. RanBPM sustains the protein stabilization of Mgl-1, and promotes its tumor suppressor activity [12]. However, the detailed mechanism underlying the effect of RanBPM on DDR of NSCLC cells remains unclear.

As a broadly acting cyclin-dependent kinase inhibitor, p21 plays a critical roles of tumor suppressor. The dysregulation of p21 has been reported in multiple human cancers [13]. In normal physiological conditions, p21 protein is rapidly degraded by the ubiquitin-proteasome pathway [14, 15]. However, in response to diverse cellular stress, such as DNA damage, the protein levels of p21 rapidly elevated, which results in cell cycle arrest, apoptosis or cellular senescence [16]. Recent studies have revealed that USP11 deubiquitinates and stabilizes p21 protein under physiological conditions, as well as in response to DNA damage [17].

In this present study, we reported a new molecular mechanism by which RanBPM sustains the protein stability of p21 in a USP11-dependent manner. In particular, we found that DNA damage promoted the ATM-mediated nuclear translocation of RanBPM protein, and colocalized and physically interacted with p21. Taken together, RanBPM has been identified as a novel regulator of p21 protein stability, and plays a critical role in the regulation of DDR.

2 Materials and methods

2.1 Cell cultures

HEK293T, A549 and H1299 cells were purchased from American Type Culture Collection (ATCC, Manassas, VA). A549 and H1299 cells were cultured in RPMI 1640 medium (Gibco, ThermoFisher Scientific, Friendship, ME, USA) supplemented with 10% fetal bovine serum (FBS, Thermo Fisher Scientific, Waltham, MA, USA) plus 5 mM glutamine, penicillin G (100 U mL^{-1}) and streptomycin (100 µg mL^{-1}) at 37 °C under 5% CO_2. HEK293T were maintained in Dulbecco's Modified Eagle Medium (DMEM) supplemented with 10% FBS and 1% penicillin/streptomycin. The experiment protocol was approved by the Ethics Committee of the Guangdong Pharmaceutical University.

2.2 Antibodies and chemicals

Specific antibodies against p53 (DO-1, sc-126), p15 (D-12, sc-271,791), p19 (SPM429, sc-65,594) and RanBPM (sc-271,727) antibodies were purchased from Santa Cruz Biotechnology (Dallas, Texas, USA), and p18 (#2896), p21 (#2947), p57 (#2557) and RanBPM (#14,638) antibody were purchased from Cell Signaling Technology (Danvers, MA, USA). Anti-p16 (A301-267 A) was purchased from Bethyl Laboratories (Montgomery, TX, USA). Anti-p27 (AF1669), anti-ATM (AF1399) and anti-phospho-ATM (Ser1981) were purchased from Beyotime Biotechnology (Shanghai, China). Anti-USP11 (ab109232) and anti-RanBPM (ab205954) antibodies were purchased from Abcam (Shanghai, China). Anti-GAPDH (AT0002) antibodies were purchased from CMCTAG (Milwaukee, WI, USA). Anti-Flag (cat. M185-3 L), anti-Myc (cat. M192-3) and anti-HA (cat. M180-3) antibodies were purchased from Medical & Biological Laboratories CO., LTD. (Minato-ku, Tokyo, Japan). Etoposide (VP-16, S1225) and KU-55,933 (S1092) were purchased from Selleck Chemicals (Shanghai, China), and Cycloheximide (sc-3508B) and MG132 (C2211) were purchased from Sigma (Shanghai, China). Doxorubicin (SC0159) was purchased from Beyotime Biotechnology (Shanghai, China).

2.3 Western blotting and immunoprecipitation

The procedures of western blotting and Immunoprecipitation assay were performed as previously described [17].

2.4 GST pulldown assays

GST fusion proteins and His fusion proteins were produced following standard protocol. For in vitro binding assays, bacterially expressed GST-p21 bound to glutathione Sepharose beads (Thermo Scientific, 16,100) were incubated with His-RanBPM. After washing, the bound proteins were separated by SDS-PAGE and immunoblotted with indicated antibodies.

2.5 Protein half-life assays

Cells were transfected with the indicated siRNA for 48 h, or transfected with specified plasmids for 24 h followed by treatment with/without cycloheximide (50 µg·mL^{-1}) for various periods of time, washed with PBS, and lysed

in RIPA buffer containing a protease inhibitor cocktail. The protein levels were assessed using Western blot analysis.

2.6 Real-time PCR

Total RNA was extracted using Trizol (Takara Bio, Otsu, Japan). RNA (1 µg) was reverse-transcribed in a 20 µL reaction using RevertAid First Strand cDNA Synthesis Kit (Thermo Scientific, #K1622). After reverse transcription at 42℃ for 60 min, then 42℃ for 15 min and inactivation by incubating samples at 70℃ for 5 min, the RT reaction was diluted. cDNA was used for RT-PCR or real-time PCR assay. Primer sequences were as follows:

RanBPM-F: GGTGATGTCATTGGCTGTTG.
RanBPM-R: AATTTGGCGGTAGGTCAGTG.
GAPDH-F: AAGGTGAAGGTCGGAGTCAA
GAPDH-R: AATGAAGGGGTCATTGATGG
p21-F: ATTAGCAGCGGAACAAGGAGTCAGACAT.
p21-R: CTGTGAAAGACACAGAACAGTACAGGGT.

2.7 RNA interference

The sequences of the RanBPM siRNAs have been previously reported:

siUSP11#1: 5'-AAUGAGAAUCAGAUCGAGUCC-3'.
siUSP11#2: 5'-AAGGCAGCCUAUGUCCUCUUC-3'.
siRanBPM#1: 5'- GGCCACACAAUGUCUAGGA-3',
siRanBPM#2: 5'-GGAAUUGGAUCCUGCGCAU-3',
and the sequence of the control siRNA is 5'-UUCUCC-GAACGUGUCACGUUUC-3'. All these siRNAs were synthesized by Shanghai GenePharma. siRNA transfection was performed in cells using GeneMut siRNA transfection reagent (SignaGen Laboratories cat. SL100568) (Rockville, MD, USA). The experimental procedure followed the protocol provided by the manufacturers.

2.8 Lentivirus transduction

To stably knock down endogenous RanBPM expression, we used a lentiviral packaging shRNA expression vector (purchased from Shanghai GenePharma) to transduce the cells. A549 cells were infected with lentivirus according to the manufacturer's instructions. The following shRNA target sequences were used: shRan-BPM: 5'-GGAATTGGATCCTGCGCAT-3' and control sequence, 5'-TTCTCCGAACGTGTCACGT-3'.

2.9 In vivo ubiquitylation assay

HEK293T cells were transfected with the indicated siRNAs, or transfected with the indicated plasmids for 24 h followed by treatment with 20 µM MG132 for 6 h, washed with PBS, and lysed in RIPA buffer containing a protease inhibitor cocktail. The lysates were transferred into a 1.5 mL tube and placed on a hot plate immediately to boil for 10 min. Then the lysates were incubated with anti-His antibody overnight, followed by treatment with protein A/G beads for an additional 2 h at 4℃. After three washes with PBS buffer containing 1‰ Tween-20 (PBST), ubiquitinated p21 was analyzed using immunoblotting with anti-HA antibody.

2.10 Clonogenic survival assay

Cells were treated with the indicated drugs, then collected, counted, diluted, then finally seeded into 6-well plate at an appropriate density for each treatment. After 10 to 14 days of incubation, the colonies were fixed and stained with crystal violet for 30 min. The colonies ($\geq$ 0.3 mm) with at least 50 cells were counted as survivors under a stereomicroscope by ImageJ software. Data are representative of three independent experiments.

2.11 Cellular fractionation

Cells were treated with DMSO, 5µM Etop or 0.5µM Dox for 8 h and harvested from the 6 cm dishes, then cell fractionation was carried out using NE-PER Nuclear and Cytoplasmic Extraction Reagents kit (cat. 78,833) according to the manufacturer's instructions. The purity of these fractions was determined using specific protein markers, namely Tubulin and RCC1, respectively.

2.12 Immunohistochemical staining analysis

Formalin-fixed, paraffin-embedded samples were sectioned at 5 µM. Sections were treated with antigen retrieval buffer. Specifically, incubation with antibodies against RanBPM (1:50 dilution; Santa Cruz, USA), p21 (1:100 dilution; CST) was carried out overnight at room temperature. Slides were incubated in secondary antibody. The protein levels of RanBPM and p21 in the tumor specimens from NSCLC patients were reviewed and scored under a light microscope. Each specimen was quantified and assigned a score based on the intensity of the membrane, cytoplasmic, and/or nucleic staining by a visual grading system (0–3) (grade 0, no staining; grade 1, weak staining; grade 2, moderate staining, grade 3, strong staining) and the extent of stained cells (0% =0, 1–24% =1, 25–49% =2, 50–74%=3, 75–100%=4). The final immunoreactive score ranges from 0 (no staining) to 12 (strong staining).

2.13 In vivo tumorigenesis study

To establish non-small cell lung cancer xenografts in nude mice, a total of 5×10^6 A549 cells expressing the indicated shRNA or constructs were stably transfected with either control, or the indicated shRNAs targeting RanBPM were harvested, washed with PBS, suspended in 100 µL of PBS, and injected into the right flank of each mouse (n = 6 per group). The treatments included the intraperitonial injection of vehicle (control group), Etoposide (10 mg/kg), or Dox (4 mg/kg). Tumor volume and body weight were checked every 3 days, and the tumor volume was calculated based on the following formula: $V = (L \times W^2)/2$, where L is the longest diameter and W represents the shortest diameter.

2.14 Survival analysis

The effects of RanBPM genes on the survival of patients with NSCLC were analyzed using Kaplan–Meier Plotter (http://kmplot.com/analysis/) [18], which contained gene expression data and survival information of 2,434 clinical NSCLC patients.

2.15 Statistical analysis

All data were analyzed by GraphPad Prism 9.0 (GraphPad Software, San Diego, CA, USA; RRID:SCR_002798) or FlowJo software (FlowJo, RRID:SCR_008520). Results are presented as mean ± SEM or mean ± SD as indicated. The statistical difference between two samples was analyzed by Students t test. One-way ANOVA was used to analyze the statistical difference of multiple groups. *P < 0.05 and **P < 0.01. P < 0.05 was considered as statistically significant.

3 Results

3.1 RanBPM is significantly downregulated, and positively correlated with p21 in NSCLC tissues

To explore the roles of RanBPM in the development of NSCLC, we performed immunohistochemical (IHC) staining using antibodies against RanBPM on the tumor tissue microarrays consisting of 82 NSCLC patient specimens. NSCLC tumor specimens express much lower RanBPM levels than the normal tissues adjacent to the tumor (Fig. 1A-B). It was reported that RanBPM knockdown induced cell cycle arrest at S-phase [9]. However, the detailed mechanism remains unclear. We analyzed the correlation of RanBPM (RANBP9) with cyclin-dependent

kinases inhibitors (CKIs) by using Gene Expression Profiling Interactive Analysis (GEPIA) web server (Fig. 1C and Figure S1A). The expression levels of RanBPM is positively correlated with p21(CDKN1A) in NSCLC tumor samples (Fig. 1D). RanBPM knockdown specifically decreased p21 level (Figure S1B). We further validated the correlation of RanBPM with p21 protein levels in NSCLC tumor specimens by IHC analysis (Fig. 1D-E). These data indicated that the expression of RanBPM is positively correlated with p21 in the tumor specimens of NSCLC patients.

3.2 RanBPM protein interacts with p21

RanBPM, as a scaffolding protein, is a crucial component of multiple-protein complex that mediate diverse cellular functions by modulating and/or assembling with various kinds of proteins [19]. Given RanBPM is positively correlated with p21, we further tested whether RanBPM protein physically interacts with p21. RanBPM or p21 was separately immunoprecipitated from the lysates of A549 cells, and the protein of p21 or RanBPM was detected by western blotting. As shown in Fig. 2A and B, both RanBPM and p21 were detected in their individual immunoprecipitated complexes, but not in the isotype-matched negative control IgG complexes. We also detected the colocalization of RanBPM and p21 proteins in the nuclei (Fig. 2C). Furthermore, the plasmids encoding Flag-RanBPM or Myc-p21 were transfected into HEK293T cells, and RanBPM or p21 protein was co-immunoprecipitated (co-IP) with an anti-Flag or anti-Myc antibody. The exogenously expressed RanBPM was pulled down by the ectopically-overexpressed p21, while the exogenously expressed p21 was pulled down by the ectopically-overexpressed RanBPM as well (Fig. 2D-E). To further validate whether RanBPM physically interacts with p21 protein, we performed GST-pull down assay by using the purified recombinant His-RanBPM and GST-p21 proteins. The GST-p21, but not the GST control, was able to pull down the His-RanBPM protein under cell-free conditions (Fig. 2F), demonstrating a direct protein interaction between RanBPM and p21. Collectively, these results suggested that RanBPM physically interacts with p21 protein in vivo and in vitro.

3.3 RanBPM stabilizes and deubiquitinates p21 protein

Since RanBPM protein physically interacts with p21, we next investigated whether RanBPM affects the steady-state levels of p21 protein. As shown in Fig. 3A, knockdown of RanBPM with two independent RanBPM specific
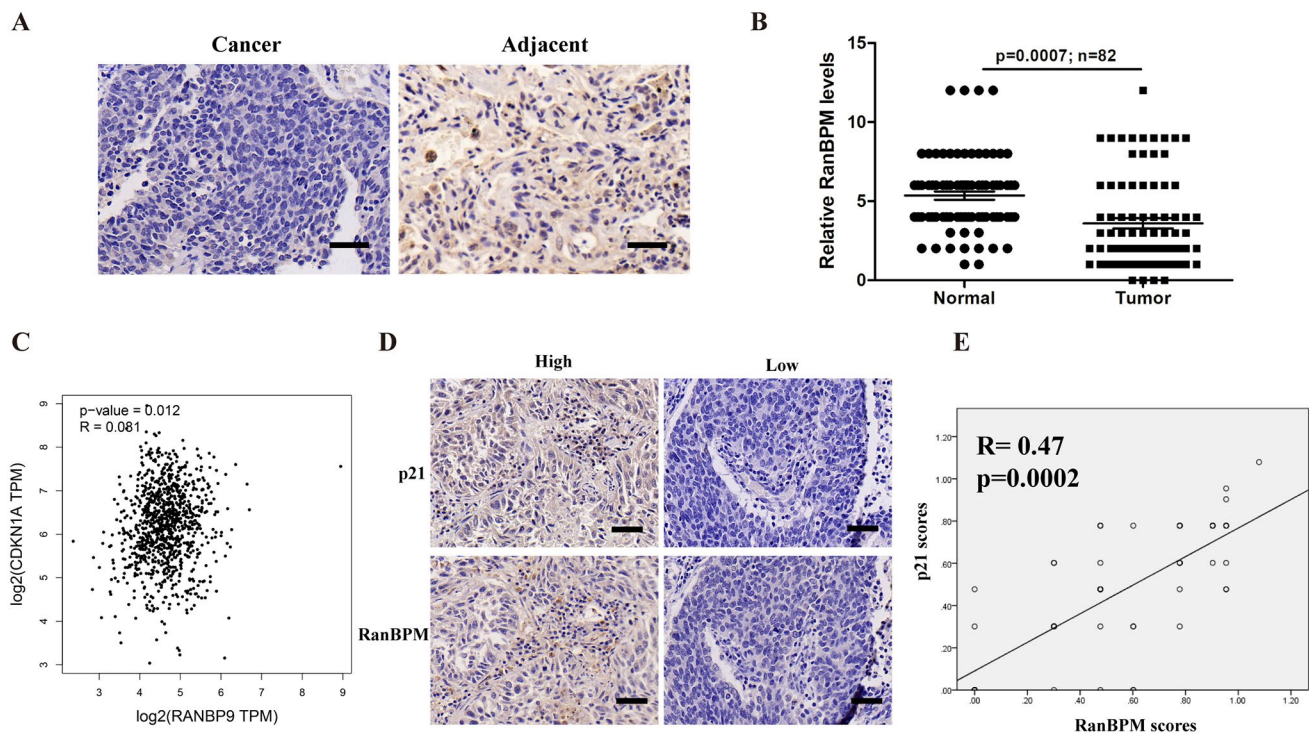
Fig. 1 RanBPM is significantly downregulated, and positively correlated with p21 in NSCLC tissues. (**A**) Representative immunohistochemical (IHC) images of RanBPM in NSCLC tissues or the matched adjacent tissues. (**B**) Quantitation of RanBPM protein levels from IHC images. (**C**) Correlation analysis of the mRNA levels of *RanBPM* and *p21* genes in NSCLC samples from TCGA datasets. (**D**) Representative IHC images of RanBPM and p21 in NSCLC tissues. (**E**) Regression analysis comparing RanBPM and p21 expression in NSCLC tissues. n = 52

short interfering RNAs (siRNAs) significantly decreased p21 level in A549 and H1299 cells. Conversely, RanBPM overexpression led to the accumulation of endogenous p21 protein regardless of the p53 status (Fig. 3B). To determine whether RanBPM regulates p21 at the level of gene transcription, we measured the mRNA levels of *p21* gene by qRT-PCR after RanBPM downregulation or overexpression. RanBPM did not significantly change the mRNA levels of *p21* (Fig. 3C-D). The data suggested that RanBPM regulates the post-translational modifications, rather than gene transcription of *p21* gene.

To further elucidate the mechanism by which RanBPM sustains the protein stability of p21, we monitored the protein degradation of p21 when the cells were treated with proteasome inhibitor MG132. In the absence of MG132, RanBPM overexpression or downregulation elevated or declined p21 protein levels in A549 or H1299 cells, while dysregulation of p21 caused by RanBPM could be blocked by the proteasome inhibitor MG132 (Fig. 3E-F). The data demonstrated that RanBPM regulates p21 protein through ubiquitin-proteasome pathway. Furthermore, when the protein biosynthesis was inhibited with cycloheximide (CHX), the knockdown of endogenous RanBPM decreased the half-life of p21

protein (Fig. 3G and H), while RanBPM overexpression profoundly extended the half-life of p21 protein (Fig. 3I). To further validate the underlying mechanism by which RanBPM regulates the protein stability of p21, we measured the levels of polyubiquitination of p21 protein by co-transfecting the plasmids encoding Myc-p21 and HA-Ubiquitin to HEK293T cells. RanBPM overexpression reduced the levels of polyubiquitylated p21 protein (Fig. 3J), whereas RanBPM knockdown significantly increased the levels of p21 polyubiquitylation (Fig. 3K).

3.4 RanBPM facilitates p21 deubiquitination in a USP11-dependent manner

It has well known that USP11 plays a key role in the maintenance of p21 protein stability [17]. Interestingly, USP11 recently has been identified as a potential binding partner for RanBPM protein [20]. We validated the protein interaction with sequential immunoprecipitation assays. The plasmids encoding Flag-RanBPM, HA-USP11 and Myc-p21 were co-transfected to HEK293T cells, and RanBPM protein was first immunoprecipitated with anti-Flag M2 agarose beads and eluted with Flag peptides. p21 proteins were secondly immunoprecipitated with anti-Myc
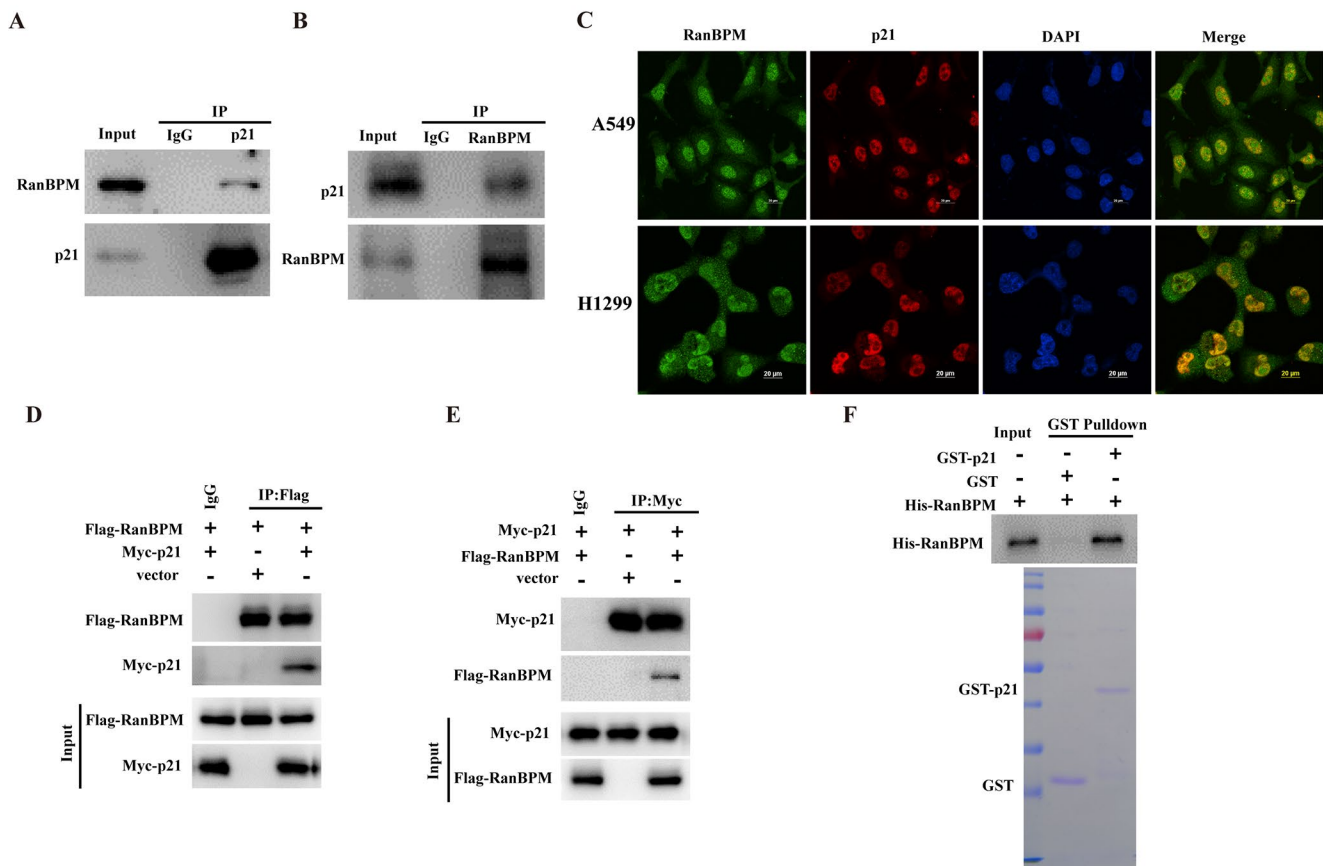
Fig. 2 RanBPM protein interacts with p21. (**A** and **B**) A549 cell lysates were subjected to immunoprecipitation with isotype control IgG, anti-p21 (**A**), or anti-RanBPM (**B**) antibody. The immunoprecipitates were then probed with anti-RanBPM or anti-p21 antibody. (**C**) The subcellular localization of endogenous RanBPM (green) and p21 (red) in A549 or H1299 cells was visualized using immunofluorescence with anti-RanBPM or anti-p21 antibody. DNA was stained with DAPI, and a merged view of the red and green channels in the same field is shown (merge). (**D** and **E**) HEK293T cells were transfected with plasmids encoding Flag-RanBPM and/or Myc-p21. RanBPM or p21 protein was individually immunoprecipitated with anti-Flag or anti-Myc antibody, and RanBPM and p21 was assessed in the immunoprecipitated complex with anti-Flag or anti-Myc antibody. (**F**) GST, GST-p21, and His-RanBPM produced from bacteria were assessed using western blotting, and the purified RanBPM protein was incubated with GST or GST-p21 coupled to GST-Sepharose. Proteins retained on Sepharose were then blotted with indicated antibodies

antibody. The data showed that USP11 was detected in the immunoprecipitated proteins with anti-Flag or anti-Myc antibody (Fig. 4A). These data indicated that RanBPM, p21 and USP11 were present in the same protein complex.

We further presumed that RanBPM might promote the interaction between USP11 and p21, and regulate USP11-dependent deubiquitination of p21. We tested the impact of RanBPM on the protein interaction of USP11 with p21. The ectopic overexpression of RanBPM promoted the protein interaction between USP11 and p21, whereas RanBPM knockdown with siRNAs significantly reduced the USP11-p21 interactions (Fig. 4B-C). Furthermore, sub-cellular localization of p21 and USP11 were further detected by immunofluorescent staining after RanBPM was knocked down in A549 cells. The knockdown of

RanBPM did not seem to change the sub-cellular localization of p21 and USP11 (Figures S2).

Because RanBPM affected the interaction of USP11 with p21, we hypothesized that RanBPM is involved in USP11-mediated regulation of p21. To address this, Flag-USP11 was transfected into RanBPM-depleted cells. As expected, the effect of USP11 on p21 markedly decreased after RanBPM knockdown (Fig. 4D). Ectopical overexpression of RanBPM dramatically promoted, whereas RanBPM knockdown decreased USP11-mediated p21 deubiquitination (Fig. 4E-F). These results suggested that RanBPM plays a vital role in USP11-mediated regulation of p21.

As well known, RanBPM is a scaffold protein without any enzymatic activity [19], we deduced that RanBPM sustains p21 protein stability depending on the deubiquitinase activity of USP11. USP11 knockdown
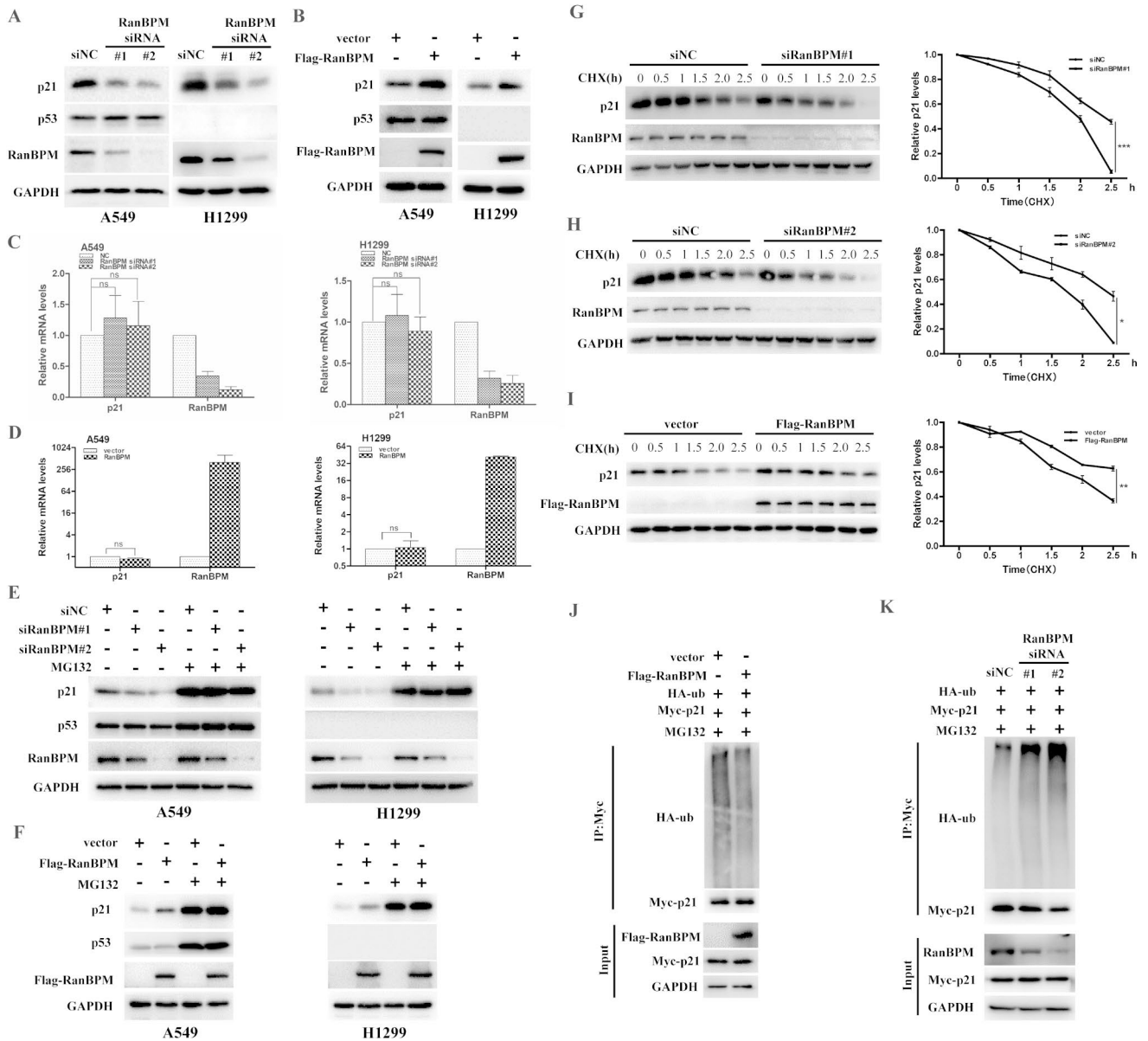
Fig. 3 RanBPM stabilizes and deubiquitinates p21 protein. (**A**) A549 or H1299 cells were transiently transfected with the indicated siRNAs, and the proteins were assessed by western blotting. (**B**) A549 or H1299 cells were transfected with the indicated plasmids, and the proteins were assessed by western blotting. (**C** and **D**) A549 or H1299 cells were infected with the indicated siRNAs (**C**), or transfected with the indicated plasmids (**D**), and the mRNA was subjected to qRT-PCR. The error bars represent the SD of triplicate measurements. (**E**) A549 or H1299 cells were transfected with the indicated siRNAs for 48 h, and then were treated with DMSO or MG132 (20 μM) for additional 6 h. The indicated proteins were analyzed by western blotting. (**F**) A549 or H1299 cells were transfected with the indicated plasmids for 24 h, and then were treated with DMSO or MG132 (20 μM) for additional 6 h. The indicated proteins were analyzed by western blotting. (**G** and **H**) A549 cells were transfected with the siRNAs of scrambled or siRanBPM#1 (**G**) or siRanBPM#2 (**H**), and then were treated with 50 μg/mL CHX. The resulting cell extracts were collected at the indi-cated time points for western blot analysis. The relative values of p21 to GAPDH expression were quantified. (**I**) A549 cells were transfected with the indicated plasmid constructs, and then were treated with 50 μg/mL CHX. The cells were collected at the indicated times, and proteins were analyzed by western blotting. The relative values of p21 to GAPDH expression were quantified. (**J**) HEK293T were transfected with plasmids encoding Flag-RanBPM, Myc-p21 and HA-Ubiquitin for 48 h, and then treated with MG132 (20 μM) for 6 h before har-vesting. p21 protein was immunoprecipitated with anti-Myc antibody, and the ubiquitination level of p21 protein was analyzed with anti-HA antibody. (**K**) HEK293T cells were transfected with the indicated siRNA for 24 h, and followed by co-transfection with Myc-p21 and HA-Ubiquitin for another 24 h. Cells were treated with MG132 (20 μM) for 6 h before harvesting. p21 protein was immunoprecipitated with anti-Myc antibody, and the p21 protein ubiquitination were tested with anti-HA antibody
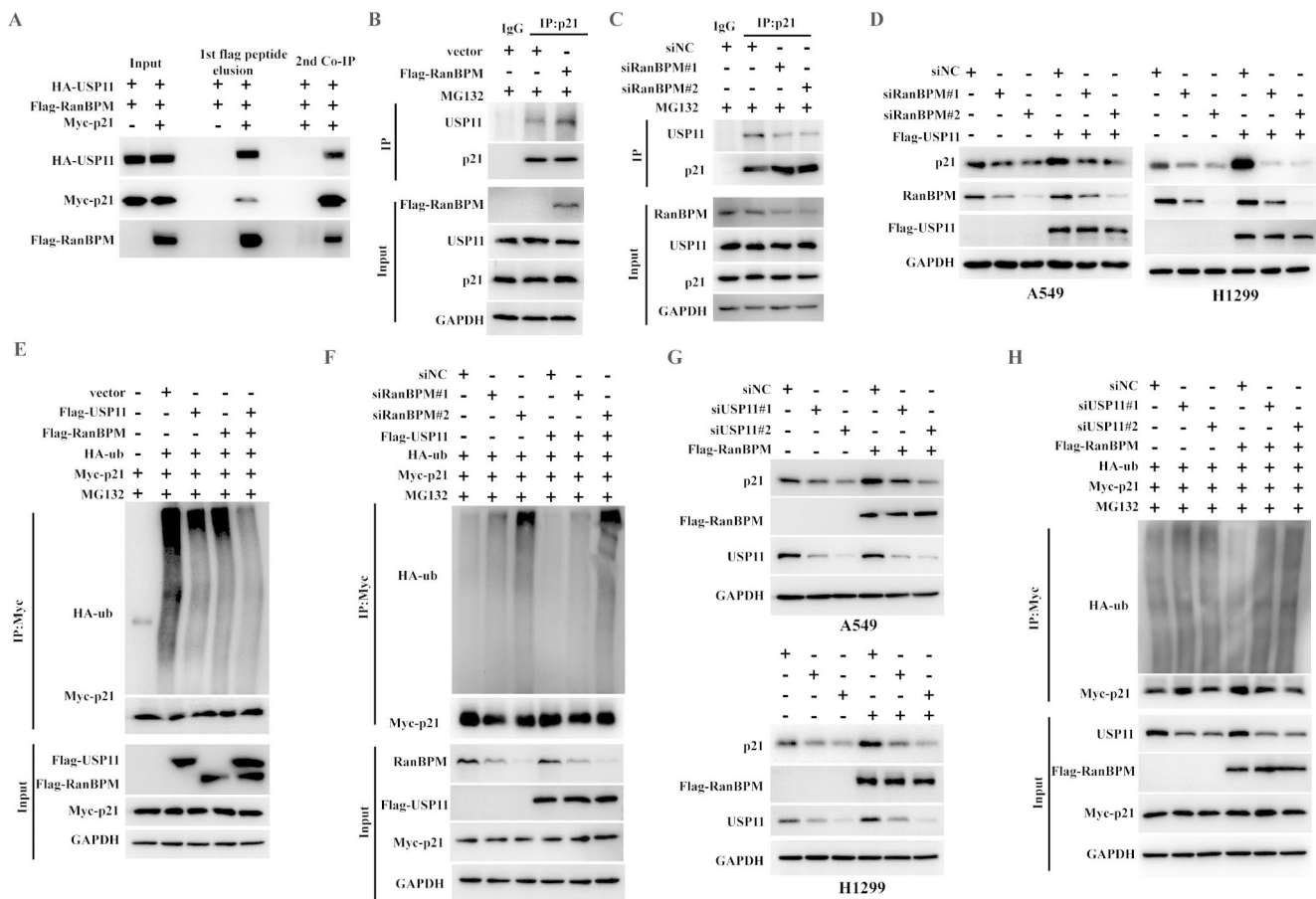
Fig. 4 RanBPM facilitates p21 deubiquitination in a USP11-dependent manner. (**A**) HEK293T cells were co-transfected with plasmids encoding Flag-RanBPM, HA-USP11 and Myc-p21, followed by MG132 treatment. Cell lysates were immunoprecipitated with anti-Flag M2 agarose beads, and eluted with Flag peptides. Eluates were further immunoprecipitated with anti-Myc or control IgG antibodies. Protein samples obtained from each step were analyzed with the indicated antibodies by western blotting. (**B** and **C**) A549 cells transfected with the indicated plasmids (**B**) or siRNAs (**C**) were treated with MG132 for 6 h. Immunoprecipitation were performed with anti-p21 antibody. The immunoprecipitates were then blotted with the indicated antibodies. (**D**) A549 or H1299 cells were transfected with the indicated siRNAs, and then were transfected with the indicated plasmid constructs. Lysates were blotted with the indicated antibodies. (**E**) HEK293T cells were co-transfected with the indicated plasmid constructs, and

followed by the treatment with MG132 for 6 h before harvesting. Cell lysates were immunoprecipitated with anti-Myc antibody, and then were analyzed by immunoblotting with anti-HA antibody. (**F**) HEK293T cells were transfected with the indicated siRNAs for 24 h, and then were transfected with the indicated plasmid constructs. Cell lysates were immunoprecipitated with anti-Myc antibody and analyzed by immunoblotting with anti-HA antibody. (**G**) A549 and H1299 cells were transfected with the indicated siRNAs, and then were transfected with the indicated plasmid constructs. Lysates were blotted with the indicated antibodies. (**H**) HEK293T cells were transfected with the indicated siRNAs for 24 h, and then were transfected with the indicated plasmid constructs. Cell lysates were immunoprecipitated with anti-Myc antibody and analyzed by immunoblotting with anti-HA antibody

significantly reduced the protein levels of p21, which has been reported in a previous study [17]. We further clarified whether RanBPM facilitates p21 deubiquitination in a USP11-dependent manner. As shown in Fig. 4G H, USP11 knockdown impaired RanBPM-sustained p21 protein stability by decreasing its deubiquitination activity. These results indicated that RanBPM stabilizes p21 protein by promoting the binding of a deubiquitinase USP11 to p21.

3.5 RanBPM regulates DNA damage response in a p21-dependent manner

A549 and H1299 cells with RanBPM knockdown showed a lower ATM activation and defective homology-directed repair (HDR), and DNA damage induced more cell apoptosis [9, 21]. To demonstrate the crucial roles of RanBPM in DDR, we measured the abilities of cell proliferation and clonogenic formation in response to genotoxic stress by using CCK-8 assays. The data indicated that RanBPM knockdown with siRNAs increased the sensitivity

of A549 to genotoxic stress (Fig. 5A-C). The rescue of exogenous p21 in the RanBPM-depleted cells fully reversed the effect of RanBPM ablation (Fig. 5D-G). These data suggested that the RanBPM-mediated DDR is dependent on p21.

To further test whether RanBPM knockdown sensitizes NSCLC xenografts to genotoxic stress in vivo,

RanBPM-depleted A549 cells were transplanted to nude mice subcutanously. The effect of RanBPM depletion on p21 protein level was validated in these xenograft tumors (Fig. 5H). Animals with similar-sized tumors were treated with Etoposide (10 mg/kg every 3 days) or Dox (4 mg/kg every 3 days). The tumor sizes were measured every 3 days. Compared to the mice transplanted with the control
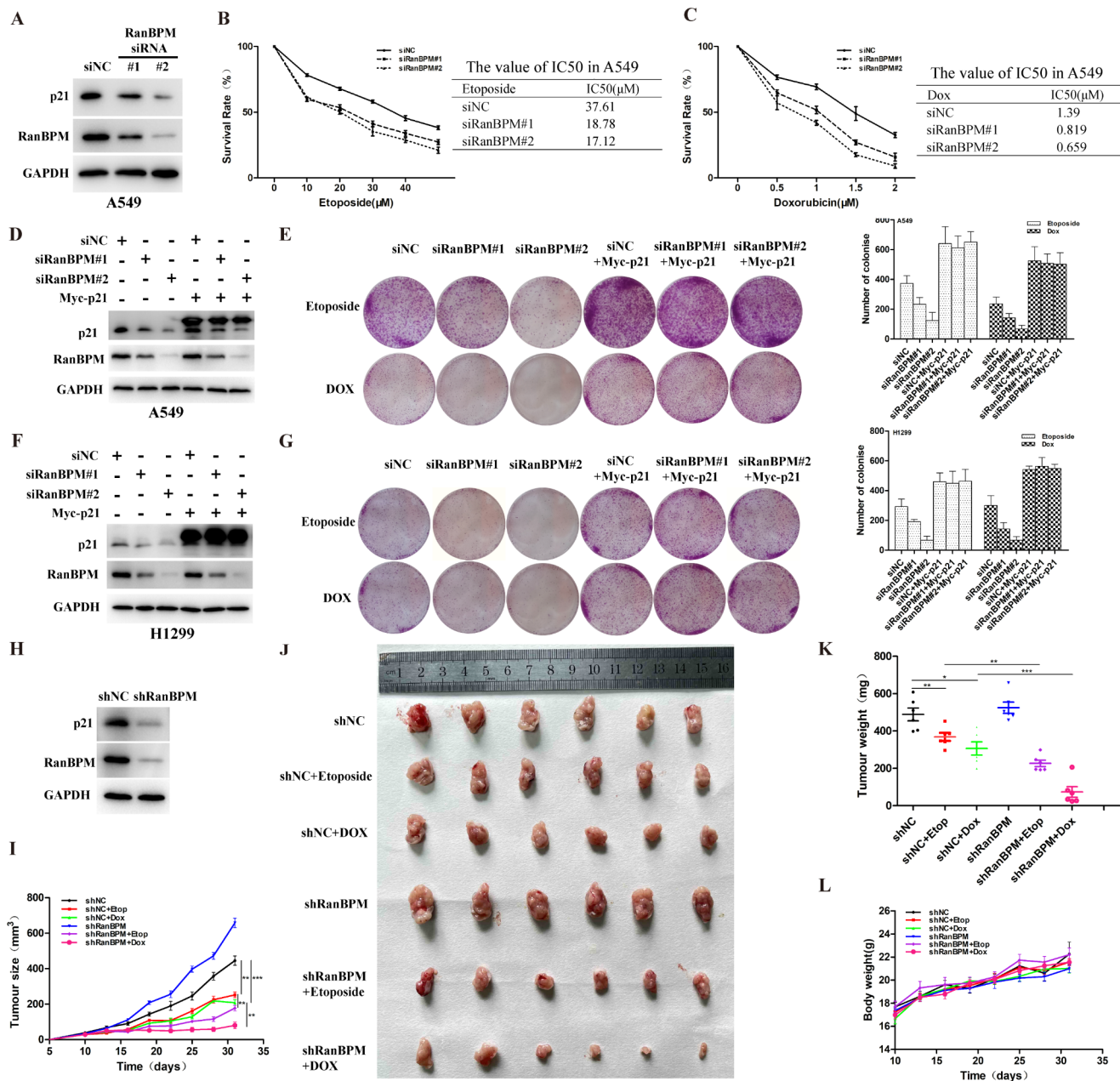
Fig. 5 RanBPM regulates DNA damage response in a p21-dependent manner. (**A-C**) A549 cells were transfected with the indicated siRNAs, and then the cells were treated with the indicated concentrations of Etop (**B**) or Dox (**C**). (**D-G**) A549 or H1299 cells were co-transfected with the indicated siRNAs and plasmid constructs, and the cells were treated with 5 μM Etop or 0.5μM Dox. The same number of cells were seeded for colony formation. Data are representative of three

independent experiments and values are expressed in mean ± SEM (***p < 0.001). (**H**) A549 cells implanted into nude mice were lysed and analyzed using Western blotting. (**I-L**) The 5×10^6 indicated shRNA-transduced A549 cells were subcutaneously injected into mice. Tumor growth (**I**), tumor images (**J**), tumor weight (**K**) and were shown

shRNA A549 cells, mice bearing the RanBPM-shRNA cells showed much faster tumor growth during the experiment (Fig. 5I). Moreover, the tumor growth curves showed that RanBPM knockdown significantly increased the sensitivity to Etoposide or Dox in tumor xenografts (Fig. 5I). The size and weight of isolated tumor nodes validated the tumor growth curve data (Fig. 5J K). Etoposide or Dox had no impact on the body weight of mice, indicating the safety of treatment at the indicated doses (Fig. 5L). The data suggested that RanBPM knockdown significantly sensitized NSCLC xenografts to genotoxic stress.

3.6 DNA damage promotes the translocation of RanBPM into the nucleus and regulates p21 protein stability

It has been reported that p21 regulates DNA damage response (DDR) by p53-dependent or independent pathways [22, 23], Since RanBPM stabilizes and deubiquitinates p21 protein, we next investigated whether DNA damage elevates p21 protein levels through RanBPM-mediated pathways. In agreement with previous reports [24], etoposide elevated p21 protein levels in A549 and H1299 cells (Fig. 6A and B), while etoposide-elevated p21 protein levels significantly decreased in the RanBPM-depleted cells (Fig. 6A). Furthermore, RanBPM knockdown significantly decreased the doxorubicin-triggered p21 elevation (Fig. 6B), but had no impact on the mRNA levels of *p21* gene (Fig. 6C and D). These results suggested that RanBPM regulates DNA damage-elevated p21 protein.

Since p21 acts as a tumor suppressor in the nucleus, we hypothesized RanBPM might translocate into the nucleus to participate in DDR. We performed cell fractionation assays or immunofluorescence to verify the hypothesis. As shown in Fig. 6E, DNA damage significantly elevated the amounts of RanBPM in the nucleus. In addition, DNA damage promoted the translocalization of RanBPM proteins to the nucleus (Fig. 6F).

Furthermore, we analyzed the physical protein interaction of RanBPM with p21. A549 cells were treated with etoposide or doxorubicin, and cell lysates were subjected to co-immunoprecipitation with anti-RanBPM or anti-p21 antibody. DNA damage significantly promoted the protein interaction between RanBPM and p21 (Fig. 6G and H). These data suggested that RanBPM is indispensable for the p21 protein stability in physiological conditions, or elevated protein levels in response to DNA damage (Fig. 6I).

3.7 DNA damage promotes the translocation of RanBPM and regulates p21 protein stability through ATM-mediated pathways

DDR induced posttranslational modifications of proteins such as phosphorylation, which are crucial for maintaining protein stability, localization and activity [25]. The DDR signaling pathway orchestrated by the ATM and ATR kinases is the central regulator of this network in response to DNA damage [26]. ATM has been reported as a binding partner of RanBPM [21]. We speculated DNA damage induced p21 protein accumulation through ATM-mediated translocation of RanBPM. Firstly, etoposide or doxorubicin up-regulated p21 protein levels in A549 and H1299 cells. However, the elevated p21 protein was remarkably decreased by ATM inhibitor Ku55933 (Fig. 7A-B). We performed cell fractionation assays to monitor the translocation of RanBPM protein. As shown in Fig. 7C, DNA damage significantly increased the amounts of RanBPM proteins in the nucleus. Intriguingly, ATM inhibition by Ku55933 reversed DNA damage-induced nuclear translocation of RanBPM. The data were validated by immunofluorescence (Fig. 7D-E). These results suggested that DNA damage significantly promoted the nuclear translocation of RanBPM protein through ATM-dependent pathways.

4 Discussion

RanBPM as a ubiquitous protein localizes in both the nucleus and cytoplasm, and has emerged as a scaffolding protein to regulate the functions of multiple binding partners by protein-protein interaction. Several studies have reported the vital roles of RanBPM in the regulation of DDR. In the present study, we reported that RanBPM sustains p21 protein stability by tethering a deubiquitinase USP11 to p21, and inhibiting p21 ubiquitination and degradation. Additionally, we also reported that RanBPM is required for DNA damage-induced p21 protein elevation, while the knockdown of RanBPM increases the sensitization of NSCLC cells to DNA damaging agents in a p21-dependent manner (Fig. 5E and G). Under normal physiological conditions, RanBPM localizes in both the cell nucleus and cytoplasm, while DNA damage promotes the nuclear translocation of RanBPM proteins in a ATM-dependent manner, thereby promoting the interaction of USP11 with p21, and stabilizing p21 protein. These results increased our understanding on the novel roles of RanBPM in the DNA damage elevates p21 protein stability, which is independent of p53 pathway.
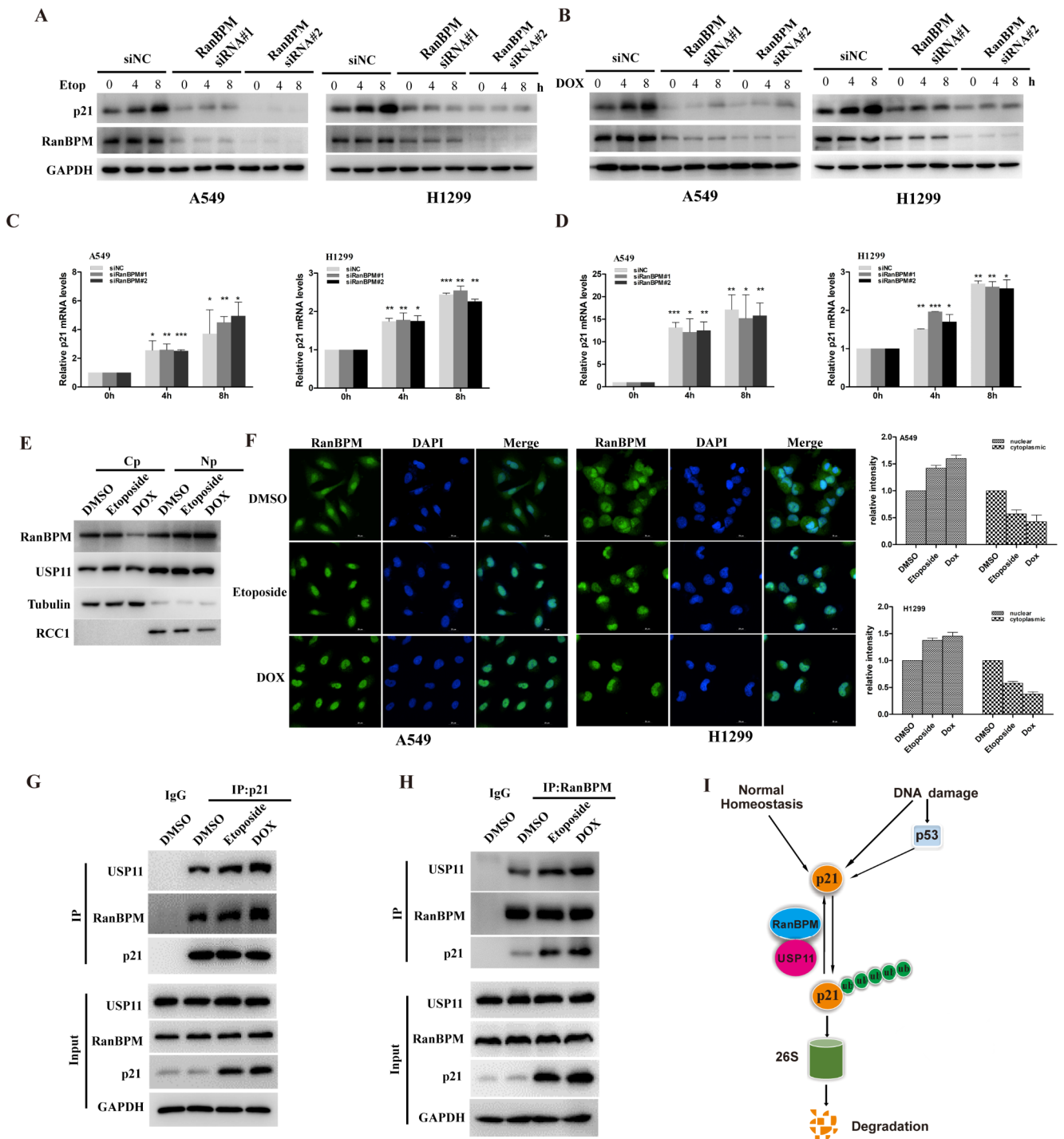
Fig. 6 DNA damage promotes the translocation of RanBPM into the nucleus and regulates p21 protein stability. (**A-D**) A549 or H1299 cells were transfected with the indicated siRNAs, and then were treated with DMSO, 5μM Etoposide (Etop) or 0.5μM doxorubicin (Dox). The cells were collected at the indicated time points, and cell lysates were subjected to western blotting (A and **B**). The mRNA was subjected to qRT-PCR (**C** and **D**). The error bars represent the SD of triplicate measurements. (**E**) A549 cells were treated with DMSO, 5μM Etop or 0.5μM Dox for 8 h. After cell fractionation, the subcellular fractions were blotted with the indicated antibodies. (Cp, cytoplasmic; Np, nuclear). (**F**) A549 cells and H1299 cells treated DMSO, 5μM Etop or 0.5μM Dox for 8 h, the cells were fixed and stained with the fluorescent anti-RanBPM antibodies. DAPI was used for nuclei staining. Scale bars, 20 μm. (**G** and **H**) A549 cells were treated with or without 5 μM Etop or 0.5 μM Dox for 8 h, and cell lysates were subjected to immunoprecipitation with control IgG, anti-RanBPM or anti-p21 antibody. The immunoprecipitates were then probed with anti-USP11, anti-p21 or anti-RanBPM antibody. (**I**) Schematic representation of p21 regulated by RanBPM-USP11 axis

Fig. 7 DNA damage promotes the translocation of RanBPM and regulates p21 protein stability through ATM-mediated pathways. (**A-C**) A549 or H1299 cells were treated with 5μM Etop or 0.5μM Dox in the presence or absence of ATM inhibitor KU-55,933 (10μM), and the total proteins were assessed by western blotting. After cell fractionation, the subcellular fractions were blotted with the indicated antibodies(**C**). (**D** and **E**) A549 or H1299 cells were treated with 5μM Etop or 0.5μM Dox in the presence or absence of ATM inhibitor KU-55,933 (10μM), and the cells were stained with the indicated fluorescent antibodies. DAPI was used for nuclei staining. Scale bars, 20 μm
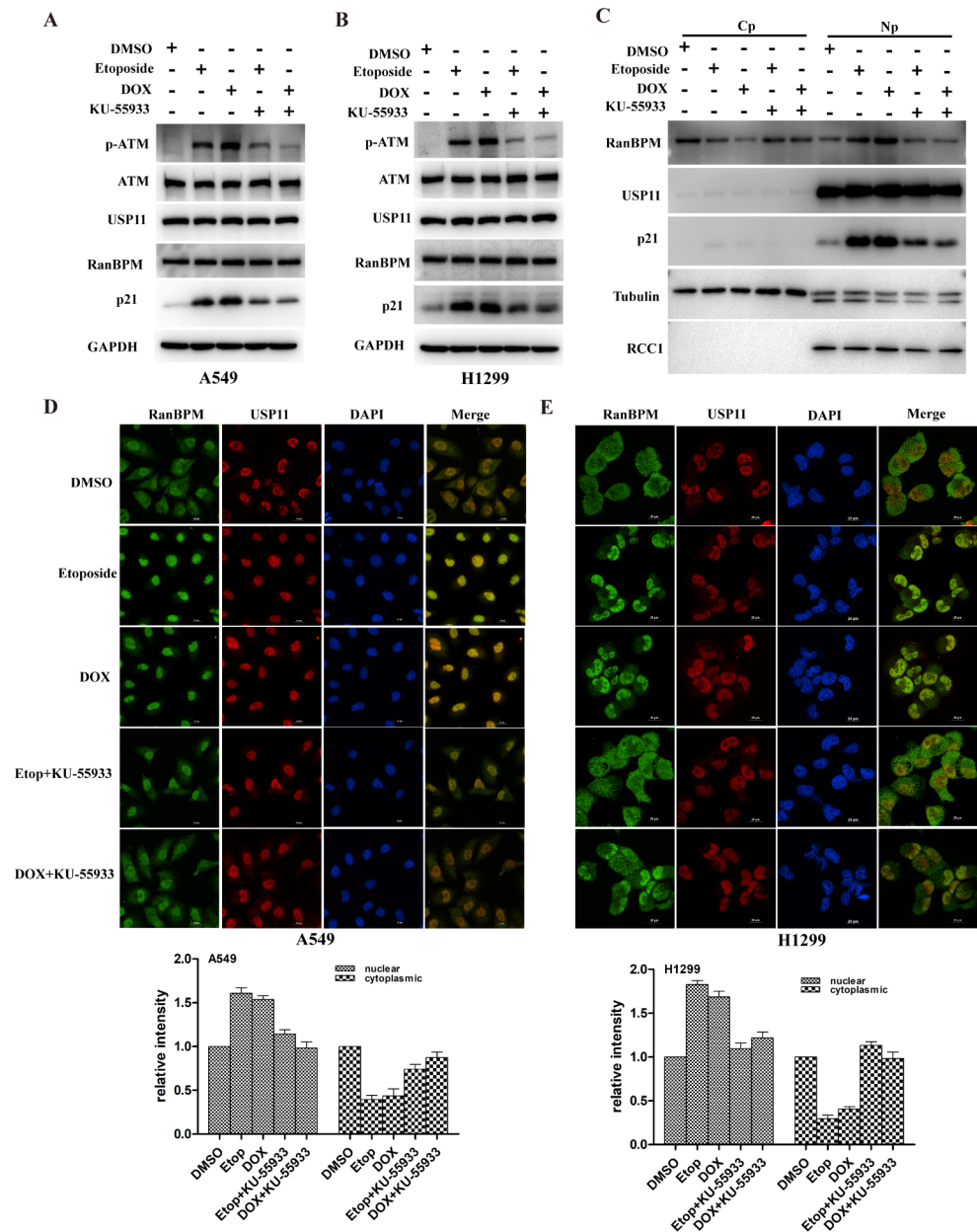
p21 is an unstable protein with a relatively short half-life, while the intrinsic and extrinsic stresses such as DNA damage or DNA replication stress rapidly elevated the protein level. The elevation of p21 protein mainly is regulated by post-translational modifications such as phosphorylation or ubiquitylation. Three E3 ubiquitin ligase complexes, SCF^{Skp2}, CRL4^{Cdt2}, and APC/C^{Cdc20}, have been reported to trigger p21 ubiquitylation and degradation at specific stages of the cell cycle. Previous study has reported that USP11 levels varies with cell cycles, and inhibits the ubiquitylation and proteasomal degradation of p21 in a cell-cycle–independent manner. Further

studies are needed to fully reveal the detailed mechanism by which RanBPM regulates p21 during cell cycle.

Altogether, the present studies demonstrated that RanBPM played a crucial role in the USP11-p21 regulatory loop when NSCLC cells were treated by DNA damage agents. DNA damage promoted the nuclear translocation of RanBPM protein, and promoted p21 protein stabilization by facilitating the interaction of p21 with a deubiquitinase USP11 (Fig. 8). The project revealed a novel mechanism by which RanBPM regulates p21 protein stability, and plays a critical role in the regulation of DDR, thereby suggesting that it might be a promising
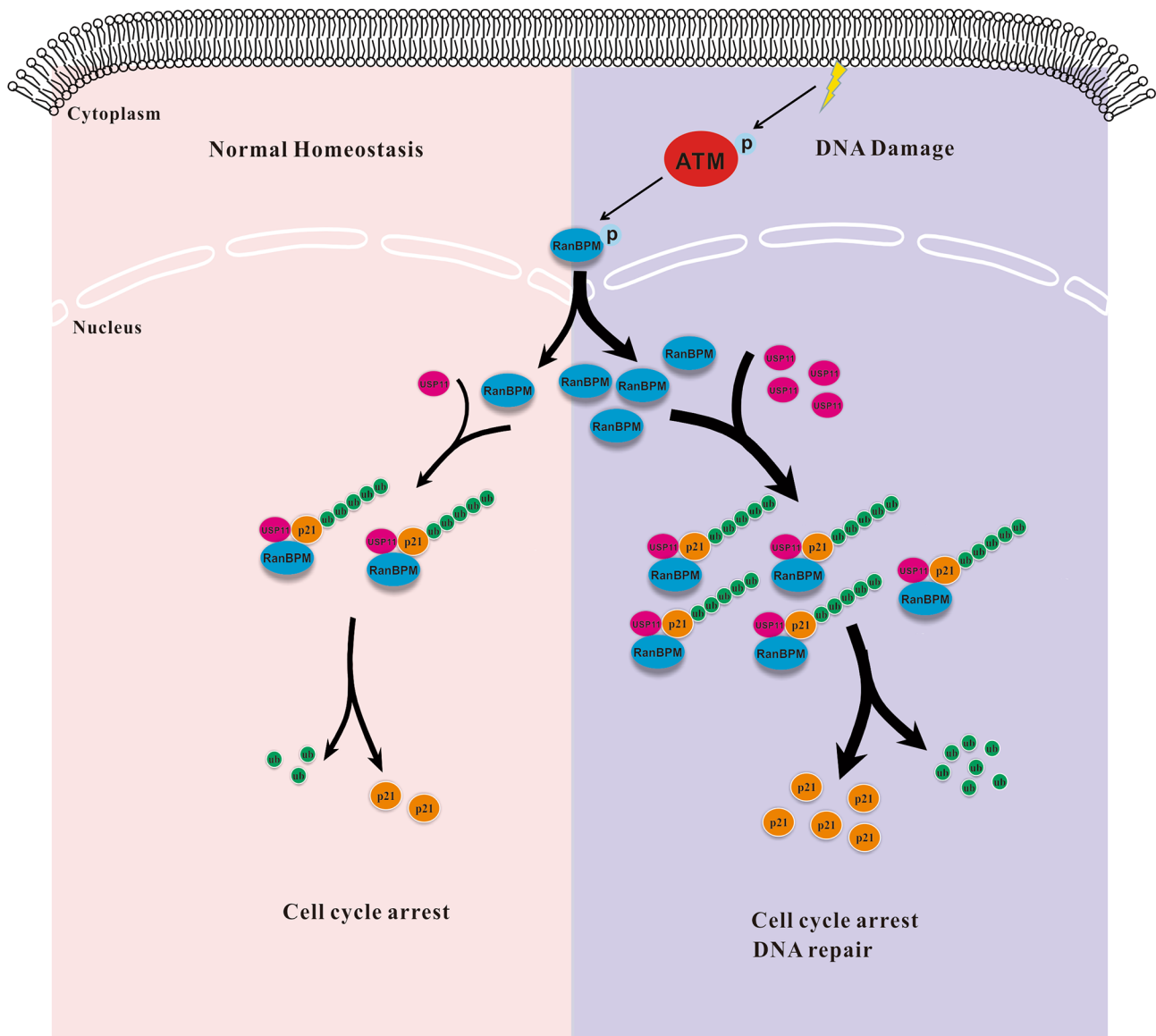
Fig. 8 Schematic representation of p21 regulated by RanBPM-USP11 axis

therapeutic strategy to develop small molecular compounds destroying the protein interaction between RanBPM and p21.

Data Availability All material and data presented in the manuscript are available.

Declarations

Ethics approval The animal study was reviewed and approved by the Use Committee for Animal Care of the First Affiliated Hospital, Guangdong Pharmaceutical University.

Consent to participate Not applicable.

Consent for publication Not applicable.

Competing interests The authors declare no competing interests.

References

1. H. Sung, J. Ferlay, R.L. Siegel et al., Global Cancer Statistics 2020: GLOBOCAN Estimates of Incidence and Mortality Worldwide for 36 Cancers in 185 Countries. CA: A Cancer Journal for Clinicians. **71**(3), 209–249 (2021)

2. Z. Chen, C.M. Fillmore, P.S. Hammerman, C.F. Kim, K.K. Wong, Non-small-cell lung cancers: a heterogeneous set of diseases. Nat. Rev. Cancer. **14**(8), 535–546 (2014)

3. A. Thomas, S.V. Liu, D.S. Subramaniam, G. Giaccone, Refining the treatment of NSCLC according to histological and molecular subtypes. Nat. Rev. Clin. Oncol. **12**(9), 511–526 (2015)

4. A. Rossi, Di M. Maio, Platinum-based chemotherapy in advanced non-small-cell lung cancer: optimal number of treatment cycles. Expert Rev. Anticancer Ther. **16**(6), 653–660 (2016)

5. D. Woods, J.J. Turchi, Chemotherapy induced DNA damage response: convergence of drugs and pathways. Cancer Biol. Ther. **14**(5), 379–389 (2013)

6. M. Nakamura, H. Masuda, J. Horii et al., When overexpressed, a novel centrosomal protein, RanBPM, causes ectopic microtubule nucleation similar to gamma-tubulin. J. Cell Biol. **143**(4), 1041–1052 (1998)

7. S. Kramer, T. Ozaki, K. Miyazaki, C. Kato, T. Hanamoto, A. Nakagawara, Protein stability and function of p73 are modulated by a physical interaction with RanBPM in mammalian cultured cells. Oncogene. **24**(5), 938–944 (2005)

8. J.A. Woo, S.E. Roh, M.K. Lakshmana, D.E. Kang, Pivotal role of RanBP9 in integrin-dependent focal adhesion signaling and assembly. FASEB Journal: Official Publication of the Federation of American Societies for Experimental Biology. **26**(4), 1672–1681 (2012)

9. A. Tessari, K. Parbhoo, M. Pawlikowski et al., RANBP9 affects cancer cells response to genotoxic stress and its overexpression is associated with worse response to platinum in NSCLC patients. Oncogene. **37**(50), 6463–6476 (2018)

10. J.P. Palavicini, B.N. Lloyd, C.D. Hayes et al., RanBP9 plays a critical role in neonatal Brain Development in mice. PloS One. **8**(6), e66908 (2013)

11. S. Puverel, C. Barrick, S. Dolci, V. Coppola, L. Tessarollo, RanBPM is essential for mouse spermatogenesis and oogenesis. Development. **138**(12), 2511–2521 (2011)

12. B. Suresh, S. Ramakrishna, Y.S. Kim, S.M. Kim, M.S. Kim, K.H. Baek, Stability and function of mammalian lethal giant larvae-1 oncoprotein are regulated by the scaffolding protein RanBPM. J. Biol. Chem. **285**(46), 35340–35349 (2010)

13. T. Abbas, A. Dutta, p21 in cancer: intricate networks and multiple activities. Nat. Rev. Cancer. **9**(6), 400–414 (2009)

14. N.A. Warfel, W.S. El-Deiry, p21WAF1 and tumourigenesis: 20 years after. Curr. Opin. Oncol. **25**(1), 52–58 (2013)

15. Z. Lu, T. Hunter, Ubiquitylation and proteasomal degradation of the p21(Cip1), p27(Kip1) and p57(Kip2) CDK inhibitors. Cell. Cycle. **9**(12), 2342–2352 (2010)

16. A. Karimian, Y. Ahmadi, B. Yousefi, Multiple functions of p21 in cell cycle, apoptosis and transcriptional regulation after DNA damage. DNA Repair. **42**, 63–71 (2016)

17. T. Deng, G. Yan, X. Song et al., Deubiquitylation and stabilization of p21 by USP11 is critical for cell-cycle progression and DNA damage responses. Proc. Natl. Acad. Sci. U S A **115**(18), 4678–4683 (2018)

18. B. Gyorffy, P. Surowiak, J. Budczies, A. Lanczky, Online survival analysis software to assess the prognostic value of biomarkers using transcriptomic data in non-small-cell lung cancer. PloS One. **8**(12), e82241 (2013)

19. S. Das, B. Suresh, H.H. Kim, S. Ramakrishna, RanBPM: a potential therapeutic target for modulating diverse physiological disorders. Drug Discovery Today. **22**(12), 1816–1824 (2017)

20. H. Ideguchi, A. Ueda, M. Tanaka et al., Structural and functional characterization of the USP11 deubiquitinating enzyme, which interacts with the RanGTP-associated protein RanBPM. Biochem. J. **367**(Pt 1), 87–95 (2002)

21. D. Palmieri, M. Scarpa, A. Tessari et al., Ran binding protein 9 (RanBP9) is a novel mediator of cellular DNA damage response in lung cancer cells. Oncotarget. **7**(14), 18371–18383 (2016)

22. K.F. Macleod, N. Sherry, G. Hannon et al., p53-dependent and independent expression of p21 during cell growth, differentiation, and DNA damage. Genes Dev. **9**(8), 935–944 (1995)

23. T. Abbas, A. Dutta, p21 in cancer: intricate networks and multiple activities. Nat. Rev. Cancer. **9**(6), 400–414 (2009)

24. H. Ding, W. Duan, W.G. Zhu et al., P21 response to DNA damage induced by genistein and etoposide in human lung cancer cells. Biochem. Biophys. Res. Commun. **305**(4), 950–956 (2003)

25. M.S. Huen, J. Chen, The DNA damage response pathways: at the crossroad of protein modifications. Cell Res. **18**(1), 8–16 (2008)

26. A. Marechal, L. Zou, DNA damage sensing by the ATM and ATR kinases. Cold Spring Harb Perspect Biol. **5**(9) (2013)